

EXTRINSIC STRENGTH MEASUREMENTS AND ASSOCIATED MECHANICAL RELIABILITY MODELING OF OPTICAL FIBER

Robert J. Castilone, G. Scott Glaesemann, Thomas A. Hanson
Corning Incorporated
Corning, NY 14831

Abstract

Strength testing was performed on over 3,800 km of fiber to obtain a distribution for use in mechanical reliability predictions. Testing on thousands of kilometers of fiber was necessary to ensure that the flaws being measured accurately represent the extrinsic flaw population of the fiber. However, due to fatigue present during any strength test, the flaws grow during the test and subsequently fail at lower stress values. Thus, the measured strength distribution appears degraded when compared to the actual post-proof test strength distribution. Using the appropriate crack growth parameters and corresponding fatigue model, the post-proof test strength of the fiber was calculated. With the proper strength distribution in place, a reliability model has been developed to predict failure probabilities for various stress events. Such events include, but are not limited to: coloring, cabling, installation, in-service lifetime, and stresses arising from events such as ice and wind exposure. Based on the results of this model, a set of safe-stress guidelines has been developed to minimize the risk of fiber failure.

Introduction

The fiber strength distribution is a key element for mechanical reliability models attempting to predict optical fiber lifetime. Ideally, one would like to have a strength distribution measured after proof testing. Figure 1 shows a flowchart demonstrating typical fiber processing steps along with the sampling of fibers for strength testing. The strength distribution should contain a sufficient length of fiber to quantify the effects of proof testing, coloring, cabling, installation, and the in-service life. This means that if thousands of kilometers of fiber are installed, thousands of kilometers should be sampled and tested. Another method for arriving at the required test length is to determine what flaws are of greatest risk for the intended application and test enough fiber to quantify the distribution of these flaws. These flaws generally fall in the extrinsic region of the schematic in Figure 2. Note that standardized methods for strength testing only test the intrinsic region of Figure 2, sampling only 15 meters of fiber.¹ Other test methods only use millimeters of fiber.² Whereas these tests are useful for scientific purposes, they do not provide sufficient data for making reliability predictions down to failure probabilities on the order of 10^{-5} to 10^{-6} .

This paper will demonstrate the proper use of a long-length strength distribution for the reliability modeling of fiber. Emphasized, will be the effects of fatigue during the strength test and how one must adjust the measured strength distribution, due to the presence of fatigue. With the proper strength distribution, used in conjunction with the model, one can predict failure probabilities for the processing steps shown in Figure 1. Examples of the model will be shown using an approach called “cascading stress events.” The Cascade model considers that flaws have the possibility of growing during all processing events. Thus, one stress event will alter the fiber strength distribution for all subsequent downstream processing events. By inputting applied stress values and durations for processing events, the Cascade model can give failure probability predictions for every step in a process or application.

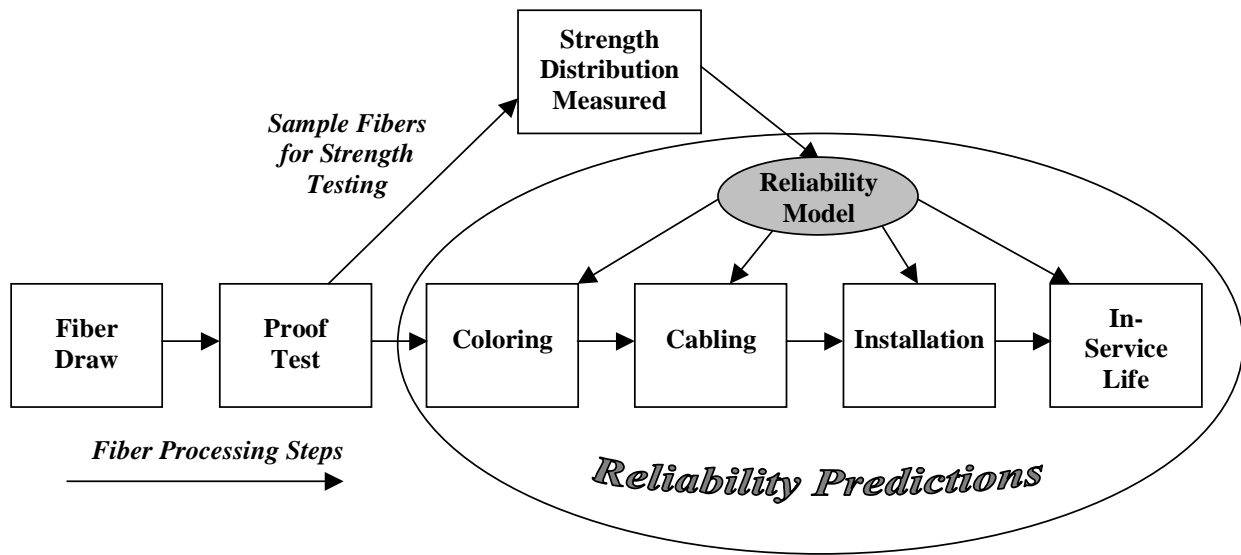


Figure 1. Flowchart showing typical fiber processing and the use of a strength distribution to model the reliability of these processing steps.

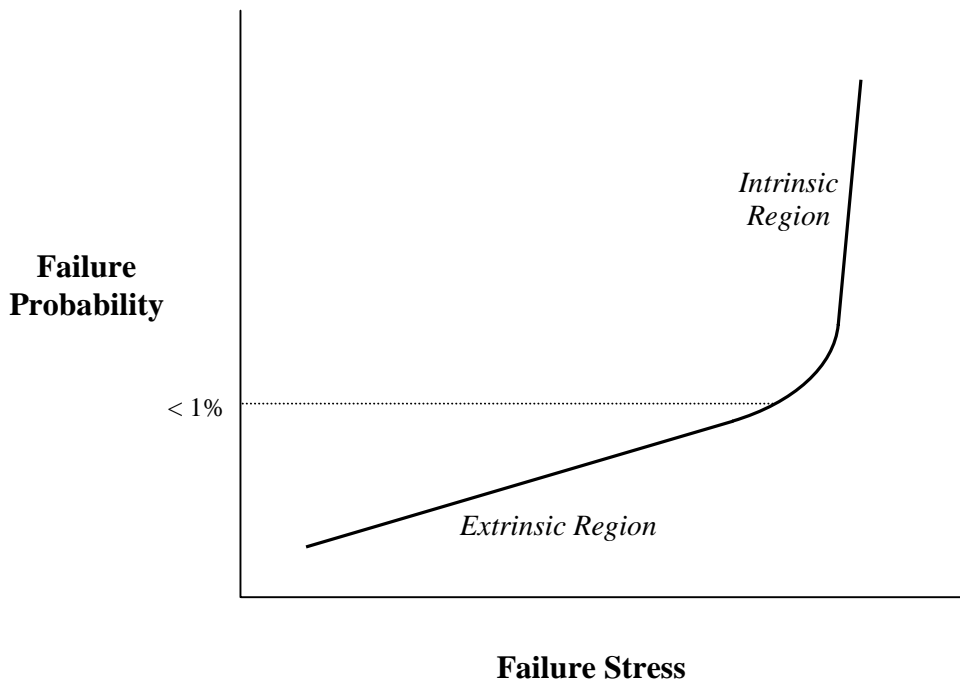


Figure 2. Schematic of a typical 20-meter gauge length fiber strength distribution.

Obtaining a Strength Distribution

There are several methods for obtaining long-length strength distributions. One could test successive ten or twenty meter lengths to failure. This method is time consuming and laborious. Multiple rescreening has been attempted in the past. With this method, one proof tests fiber over a range of stress levels. By counting the breaks at each level, one can calculate the failure probability for each stress level. Whereas this method more efficiently tests many kilometers of fiber in a relatively short period of time, it is difficult to quantify subtleties in the curvature of the strength distribution.

Several years ago a novel suspended test method was created for obtaining long-length strength distributions. A schematic of the long-length strength testing equipment is shown in Figure 3. The details surrounding this test have been previously published.³ In the test, sequential 20-meter sections of fiber are elongated to a load of 350 kpsi (2.41 GPa). A load cell monitors the load as the stress is being applied. If a break does not occur, another 20 meter length is indexed and the load is again applied to the next section of fiber. The rate at which the load is applied is set to approximately 200% elongation per minute. When a break occurs, the break stress is recorded. Testing of multiple reels of fiber is performed until enough breaks are recorded to accurately describe the region between the proof test and the 350 kpsi limit. Flaws passing the stress pulse are generally not of reliability concern. The rarity of low strength flaws means that long-lengths of fiber can be searched relatively quickly.

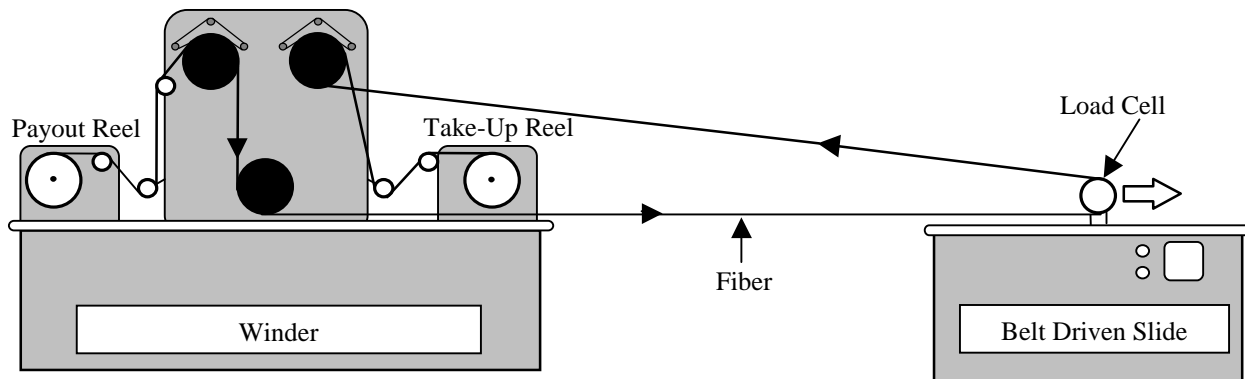


Figure 3. Schematic of the long-length extrinsic strength tester.

Previous publications of strength distributions containing hundreds of kilometers of fiber were performed on fiber proof tested at only 50 kpsi (0.34 GPa), the standard level at the time.³ These distributions were published nearly a decade ago on an older vintage of fiber. In this study, nearly 4000 kilometers of standard single-mode fiber was strength tested using the test method described above. This fiber was proof tested at 100 kpsi (0.7 GPa) in accordance with FOTP-31C.⁴ The measured results from this strength testing are shown in Weibull fashion as the triangles in Figure 4. Note that only the weakest flaws, those below 350 kpsi, are loaded to failure. The flaws that pass the test are accounted for statistically. For this reason, only failure probabilities below 0.01 are shown in the plot.

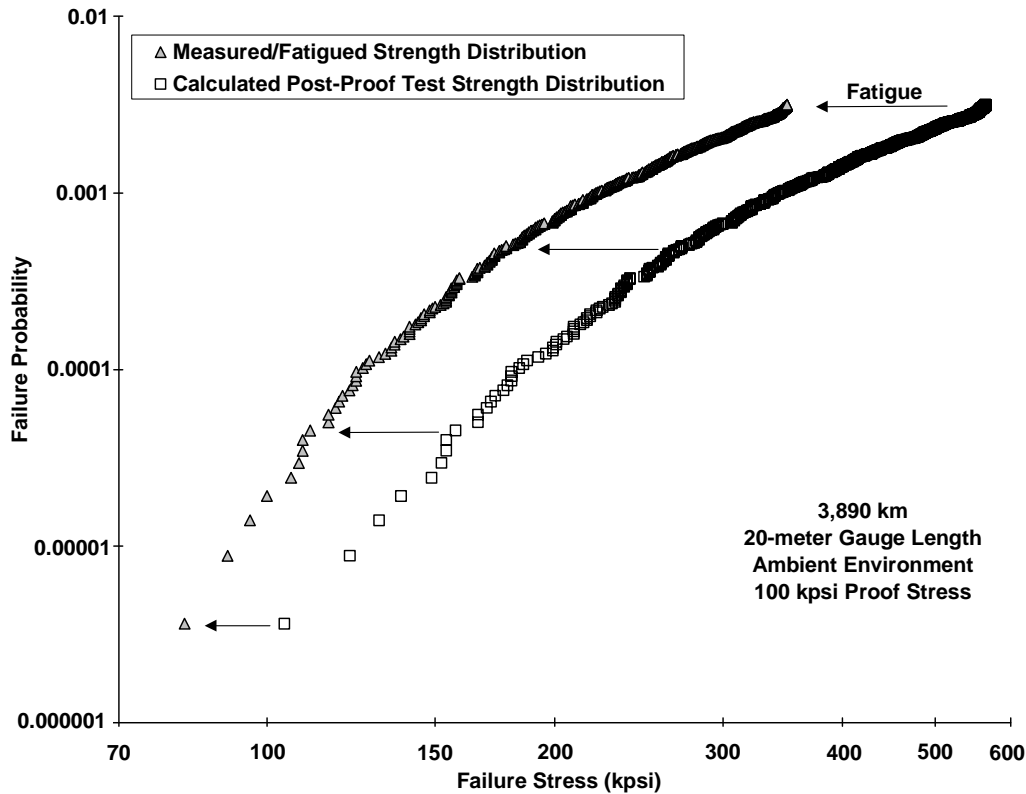


Figure 4. Weibull plot showing how fatigue can reduce the measured strength distribution of fiber.

A feature of any proof-tested fiber is the truncation of the strength distribution near the proof stress level. This truncation occurs statistically as flaws which have been eliminated by the proof test. The measured data shown in Figure 4 appears to truncate to a stress level below the actual proof stress. However, as mentioned above, the test was performed at a finite strain rate of 200%/minute which fatigues the flaws to lower strength values.

The problem with all long-length strength test methods is that they must be performed in fatigue environments. This means that while loading the fiber to failure, the fiber strength degrades somewhat from its pretest strength. For example, take a flaw which passes the 100 kpsi proof test, and has a surviving strength of 120 kpsi. A strength test after proof testing is performed to obtain the post-proof test strength distribution, and this flaw degrades 30 to 40 kpsi during the test. Thus, the measured strength is lower than the post-proof test strength. In order to generate an accurate post-proof test strength distribution, one must account for this fatigue during strength testing. Note that the strength degradation is not a result of proof testing, rather fatigue during post-proof test strength measurements.

Figure 5 contains recent data showing measured strength values (closed circles) for abraded fiber at varying stress rates.⁵ The open circles represent the calculated initial strength of the fibers in the absence of any fatigue. With the faster stressing rates, the strength approaches the predicted initial strength. However, as indicated on the plot, the strength values for 200%/min. rate (400 kpsi/sec.) used during the long-length strength test are well below the predicted initial strength values. This indicates that significant fatigue has occurred during the strength test.

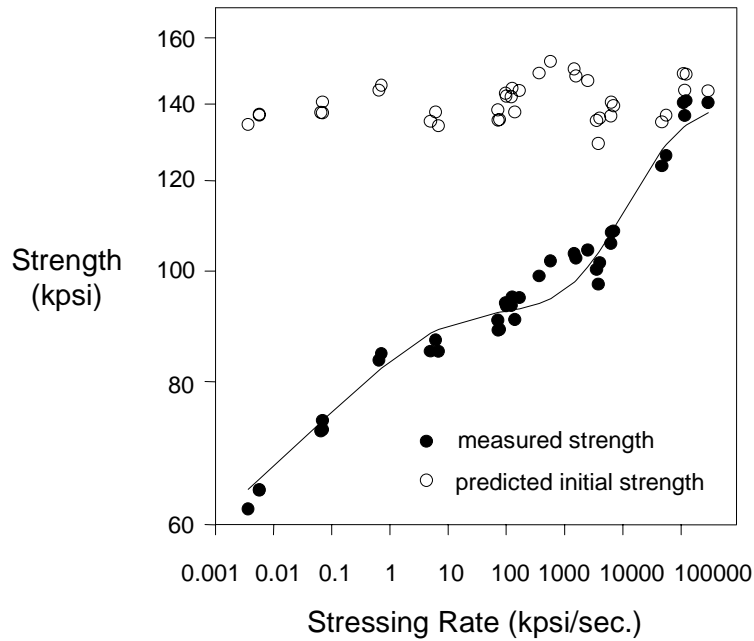


Figure 5. Predicted initial strengths and measured strengths on abraded fiber. The predicted measured strength using this model is shown as a line.

The line in Figure 5 is the predicted fatigue strength based on the crack growth model in reference six.⁶ This means that crack growth during strength testing can be accounted for. Using this model, the initial post-proof test strength distribution was calculated from the measured data in Figure 4. The squares in Figure 4 represent this calculated post-proof test strength distribution. As expected, the calculated distribution truncates at the 100 kpsi proof stress level. When this calculated distribution is compared with the measured strength distribution, the effects of fatigue during the test can be observed. It is essential that all models adjust for fatigue, as done here, to be used for reliability calculations.

Use of Initial Long-Length Strength Distribution for Reliability Predictions

All processing events can have an effect on the strength distribution, due to the possibility of fatigue. However, these events are not independent from each other. Using what we call a “cascade” approach, the strength distribution for a given stress event is influenced by all prior stress events. Each stress event may fatigue the fiber, thus affecting the beginning flaw size for the next event.

The first stress event in a fiber's life is the proof test. Proof testing is performed at high stress rates to minimize fatigue. Figure 6 shows the strength distribution after proof testing, along with the predicted distribution prior to the proof stress. This clearly shows how a cumulative probability distribution is truncated by the elimination of flaws below the proof stress.

The strength distribution can degrade with every subsequent stress event beyond proof testing, until failures occur. Figure 7 is a schematic illustrating fiber strength degradation for sequential stress events that are severe enough to generate flaw growth. Notice, how the final strength of the flaw in the installed cable depends on the applied stress and duration of each stress event including proof-testing. Fatigue can also occur during the lifetime of the fiber under stress. The ultimate goal is to ensure that the two lines do not cross, thereby, avoiding mechanical failure.

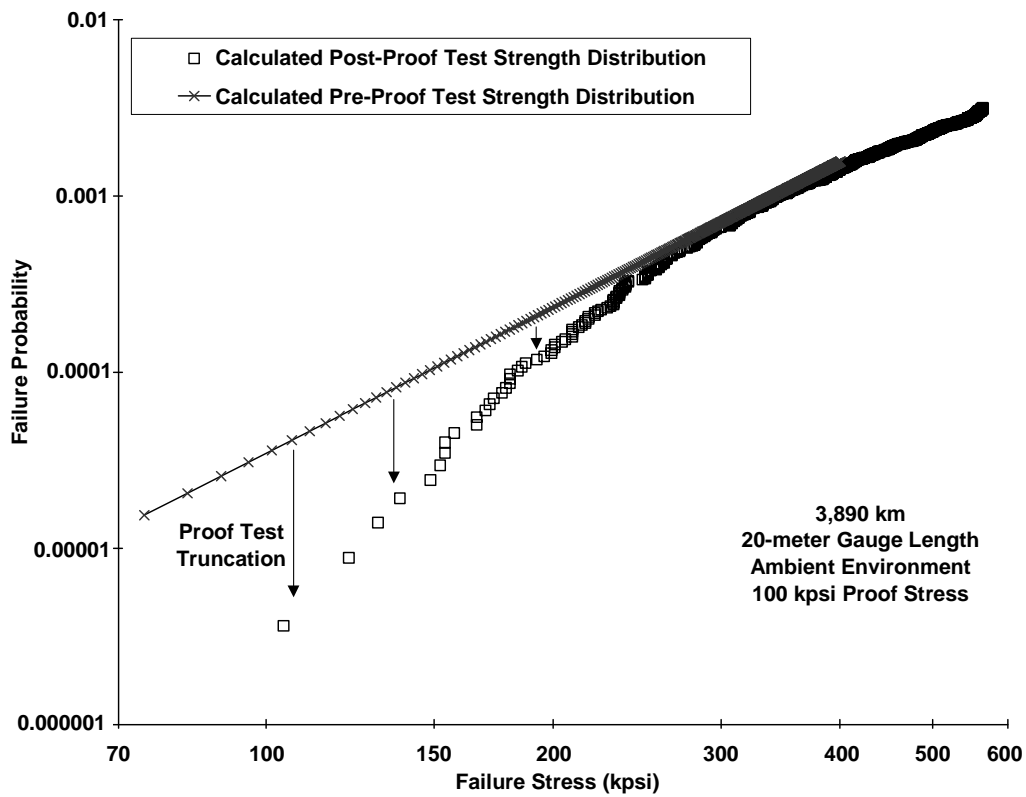


Figure 6. Plot showing the effect of the proof stress truncating the strength distribution.

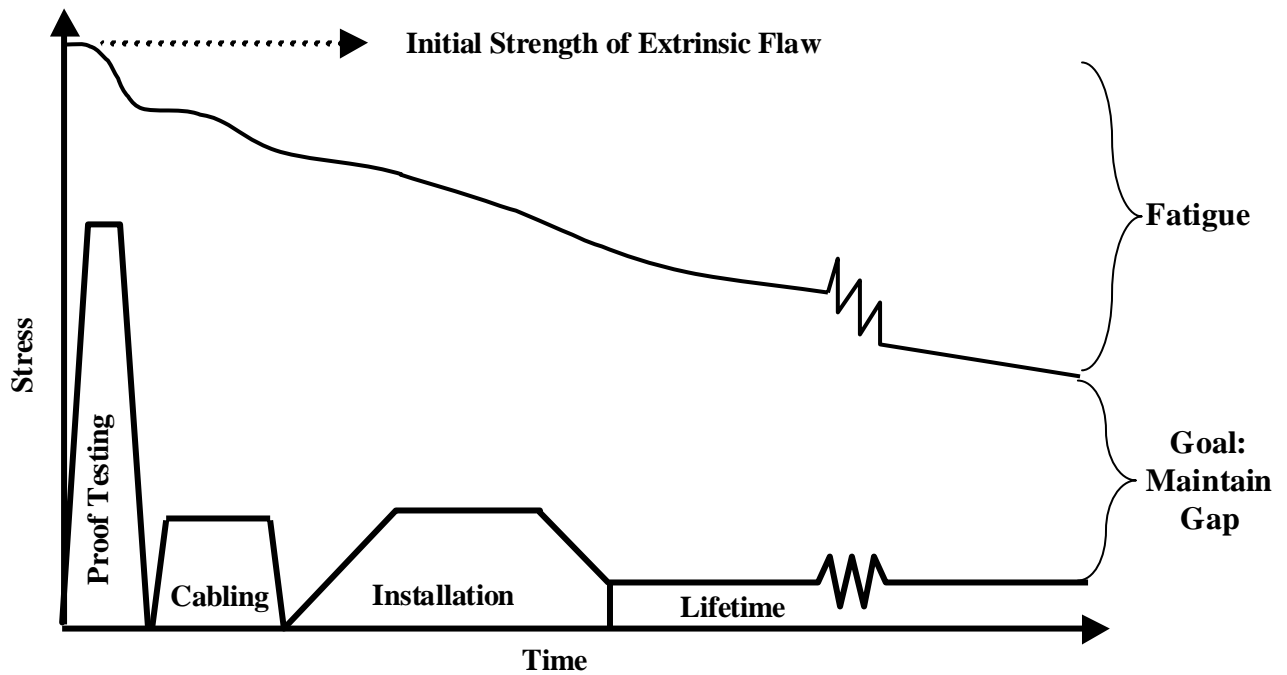


Figure 7. Schematic showing how stress events can reduce the strength of extrinsic flaws.

To minimize the risk of fiber failure during stress or lifetime events due to fatigue, a set of safe-stress guidelines have been developed. These guidelines are shown in Tables I and II for long-lengths and medium-lengths, respectively. The basic guideline for long-term in-service life, shown in Table I, is an applied stress no greater than 1/5th the proof stress. Stresses during the installation are allowed to be higher than those during in-service life, due to the shorter time period under stress. During processing, the duration of applied stress is usually short, on the order of seconds, allowing even higher applied stresses. The allowable stress guideline becomes more liberal when contrasting short-length installations (≤ 300 m) to long-length installations, as shown in Table II. This is due to the fact that short length applications have a reduced probability of encountering flaws near the proof stress level. Safe bend conditions are shown in Table III. Rows 1 and 2 of Table III are applicable to fiber in cable. Row 3 is for long fiber lengths in bending for a short period of time like that experienced during processing over pulleys. The last row of Table III shows the allowable condition for short fiber lengths in bending. In this case the allowed minimum bend radius is greatly influenced by the lack of flaws. The case for short lengths in bending may be used to determine allowable splice enclosure dimensions, for example. Again, the ability to make these determinations is predicated on having the long-length strength distribution shown in Figure 4.

Table I. Total allowable stress design guidelines for any length, resulting in zero predicted failures.

Duration of Applied Stress	Allowable Safe Stress in Relation to σ_p	Allowable Safe Stress (kpsi) when $\sigma_p = 100$ kpsi
40 years	1/5 σ_p	20 kpsi
4 hours	1/3 σ_p	33 kpsi
1 second	1/2 σ_p	50 kpsi

σ_p is the proof stress

Table II. Allowable stress guidelines for medium lengths (≤ 300 m) in tension resulting in < 1 ppm predicted failures.

Duration of Applied Stress	Allowable Medium Length Safe Stress (kpsi) when $\sigma_p = 100$ kpsi
40 years	21 kpsi
4 hours	35 kpsi
1 second	57 kpsi

Table III. Allowable stress design guidelines for various lengths in bending.

Length of Fiber	Length of Time	Risk of Failure	Minimum Bend Radius ($\sigma_p = 100$ kpsi)
> 1 km	40 years	0	30 mm
> 1 km	4 hours	0	20 mm
> 1 km	1 second	0	13 mm
≤ 5 m	40 years	< 1 ppm	25 mm

Use of Model to Predict Failure Rates in Stressing Events

Table IV demonstrates how the model is used to predict failure probabilities for a hypothetical cabling and installation process. The standard 100 kpsi fiber strength distribution was used for this scenario. Inserted into the model is a description of the stress event including: stress, dwell time at that stress, and unload time. For the safe-stress conditions listed on the left in Table IV, we predict zero failures during processing events, and during the lifetime of the fiber.

On the right side of Table IV are listed some unsafe-stress conditions. A cabling stress of 60 kpsi was introduced, well above the recommended safe-stress of 33 kpsi, for short-term events. With this elevated stress, one predicts a break rate of 0.8 breaks for every 1,000 kilometers cabled. Also listed is an in-service stress of 30 kpsi, well above the recommended safe-stress of 20 kpsi, for long-term events. This installed stress would result in approximately 0.3 breaks for every 1,000 kilometers during the lifetime of the fiber.

The model can also be used to predict stress events that arise during the lifetime of the fiber. These types of events may include ice loading or excessive stress from wind. Such events can place short-term stresses on the fibers, which may exceed the safe-stress limits. These events can be modeled during the design phase to determine the impact of such events, or even show how an elevated proof-stress level can minimize the failure probability.

Table IV. Example of safe and unsafe stresses for long-length processing and lifetime stress events.

Stress Event	SAFE STRESS				UNSAFE STRESS			
	Stress (kpsi)	Dwell Time	Unload Time (sec)	Failure Rate (Brks/kkm)	Stress (kpsi)	Dwell Time	Unload Time (sec)	Failure Rate (Brks/kkm)
Coloring	20	0.5 sec.	0.0025	0	20	0.5 sec.	0.0025	0
Cabling	25	60 sec.	1	0	60	60 sec.	1	0.787
Installation	30	4 hr.	1	0	30	4 hr.	1	0
Lifetime	20	40 yr.	1	0	30	40 yr.	1	0.284

Conclusions

The mechanical reliability modeling of optical fiber requires that one have knowledge of the frequency and size of the flaws present in the fiber. This can only be done by measuring the strength of thousands of kilometers of fiber. However, once the long-length strength distribution is measured, one must account for fatigue during the strength test. Using fatigue theory, the post-proof stress strength distribution can be calculated for use in the reliability model.

The model has been used for failure probability prediction for many different stress events. Processing events such as proof testing, coloring, cabling, and installation can be analyzed. Each processing event has potential to fatigue the fiber, provided the applied stress and its duration are sufficient to grow flaws. The amount of fatigue is determined by a combination of the applied stress level, dwell time, and unload time. For each stressing event, the model predicts the total fatigue that has occurred to determine the probability of a fiber failure during the event. Therefore, degradation of the strength distribution during one processing step affects all subsequent processing events.

To ensure a 40-year lifetime of installed fiber, a set of safe-stress guidelines has been proposed. To minimize the risk of fiber failure during long-length applications, one should not exceed 1/5th the proof test for long-term stresses. The allowable safe-stress can be increased to 1/3rd the proof stress for shorter applications, lasting under four hours. A set of guidelines has also been developed to minimize the stresses during bending applications. These guidelines were implemented to minimize failures during the processing of the fiber and to prevent fibers from being installed which pose a mechanical reliability risk in the field.

Acknowledgements

The authors would like to thank Dan Hill, Dick Kelly, Kathleen Shappee, and Jamie Westbrook for their help with the strength testing and the generation of this report.

References

1. TIA/EIA-455-28C, Measuring Dynamic Strength and Fatigue Parameters of Optical Fiber by Tension, (Telecommunications Industry Association, Arlington VA, 1999).
2. IEC 793-1-B7B, Dynamic Fatigue Parameters of Optical Fibers by Two Point Bending, (International Electrotechnical Commission, 1995).
3. G. S. Glaesemann and D. J. Walter, "Method for Obtaining Long-Length Strength Distributions for Reliability Prediction," *Opt. Eng.* **30** [6] 746-748 (1991).
4. TIA/EIA-455-31C, Proof Testing Optical Fibers by Tension, (Telecommunications Industry Association, Arlington VA, 1995).
5. P.T. Garvey, T.A. Hanson, M.G. Estep, G.S. Glaesemann, "Mechanical Reliability Predictions: An Attempt at Measuring the Initial Strength of Draw-Abraded Optical Fiber using High Stressing Rates," Proceedings of the 46th International Wire and Cable Symposium, 883-888, Philadelphia, PA, 1997.
6. T. A. Hanson and G. S. Glaesemann, "Incorporating Multi-Region Crack Growth into Mechanical Reliability Predictions for Optical Fiber," *J. Mat. Sci.*, **32**, 5305 - 5311 (1997).